ChemPubSoc Europe

DOI: 10.1002/cmdc.201300357

# Inhibition of Hypoxia-Induced Gene Transcription by Substituted Pyrazolyl Oxadiazoles: Initial Lead Generation and Structure–Activity Relationships

Michael Härter,*[a] Karl-Heinz Thierauch,[b] Stephen Boyer,[c] Ajay Bhargava,[c] Peter Ellinghaus,[d] Hartmut Beck,[a] Susanne Greschat-Schade,[e] Holger Hess-Stumpp,[b] and Kerstin Unterschemmann[b]

The transcription factors hypoxia-inducible factor-1 and -2 (HIF-1 and HIF-2) orchestrate a multitude of processes that allow tumor cells to survive under conditions of low oxygen and nutrients, and that lead to resistance to some apoptotic pathways and facilitate invasion and metastasis. Therefore, inhibition of transactivation by HIF has become an attractive target in cancer research. Herein we present the results of a cell-based screening approach that led to the discovery of substituted 1*H*-pyrazole-3-carboxamides. Chemical optimization of the hit class with respect to potency and metabolic stability is described; it resulted in novel 5-(1*H*-pyrazol-3-yl)-1,2,4-oxadiazoles that inhibit the hypoxia-induced accumulation of HIF-1α and HIF-2α. The HIF inhibitory potency in the screening cell system was improved from $IC_{50}$ 190 to 0.7 nM, and significant parts of the SAR are disclosed. For a key compound, the ability to suppress the hypoxia-induced expression of HIF target genes was studied in A549 human lung adenocarcinoma cells. The same compound shows a favorable pharmacokinetic profile in rats after i.v. and p.o. administration.

A common feature of growing tumors are areas of transient and chronic hypoxia, in which tumor cells are distant from a supportive blood vessel and thus suffer from a lack of oxygen (as well as nutrients and the removal of metabolic waste). It has been recognized that hypoxic tumor cells are often resistant to chemo- and radiotherapy and give rise to a more invasive tumor type. Clinically, tumor hypoxia is associated with aggressive disease and poor prognosis.[1] The adaptation of tumor cells to their hostile hypoxic environment is orchestrated mainly by the action of the transcription factors hypoxia-inducible factor-1 and -2 (HIF-1 and HIF-2).[2] The heterodimeric transcription factors consist of a constitutively expressed HIF-1β subunit (also called ARNT) and one of the highly regulated HIF-1α or HIF-2α subunits. Although constantly synthesized, the α subunits undergo rapid degradation in well-oxygenated tissue (normoxic conditions), a process that starts with oxygen-dependent hydroxylation of specific proline residues of the HIF-1α/2α proteins, catalyzed by prolyl hydroxylases (most importantly PHD-2), followed by binding to the von Hippel–Lindau (VHL) E3 ligase, which marks HIF-1α/2α proteins for proteasome-mediated degradation.[3] Prolyl hydroxylase activity is decreased under hypoxic conditions, leading to an accumulation of HIF-1α and HIF-2α, which translocate into the nucleus where they heterodimerize with HIF-1β and induce the transcription of HIF target genes by binding to so-called hypoxia-response elements in their respective promoter regions.[4] It is the action of the protein products of the HIF target genes that leads to the profound changes observed in hypoxic tumor cells: shift from mitochondrial respiration to glycolysis for ATP production, altered catabolism to maintain cell proliferation, induction of angiogenesis, facilitation of invasion and metastasis, and suppression of certain apoptotic mechanisms.[5] Therefore, the HIF pathway has become an attractive target in anticancer research, and a number of compounds have been reported recently that modulate HIF target gene expression by various molecular modes of action.[6] Of the compounds that can be regarded as rather specific HIF inhibitors, only EZN-2968 is currently under evaluation in clinical studies (phase 1). EZN-2968 is a locked nucleic acid (LNA) antisense oligonucleotide that targets HIF-1α mRNA.[7]

We set out to identify novel HIF pathway inhibitors by screening our company's compound collection, using the human colorectal carcinoma cell line HCT-116 stably transfect-

[a] *Dr. M. Härter, Dr. H. Beck*
*Department of Medicinal Chemistry*
*Bayer HealthCare Pharmaceuticals, Global Drug Discovery*
*Postfach 101709, 42096 Wuppertal (Germany)*
*E-mail: michael.haerter@bayer.com*

[b] *Dr. K.-H. Thierauch, Dr. H. Hess-Stumpp,[+++] Dr. K. Unterschemmann[+++]*
*Therapeutic Research Group, Oncology*
*Bayer HealthCare Pharmaceuticals, Global Drug Discovery*

[c] *Dr. S. Boyer,[+] Dr. A. Bhargava[++]*
*Former Exploratory Research Group, Small Molecules Cancer*
*Bayer Pharmaceuticals (USA)*

[d] *Dr. P. Ellinghaus*
*Biomarker Research Group, Clinical Science*
*Bayer HealthCare Pharmaceuticals, Global Drug Discovery*

[e] *Dr. S. Greschat-Schade[+++]*
*Research Pharmacokinetics Group*
*Bayer HealthCare Pharmaceuticals, Global Drug Discovery*

[+] *Current address: Bristol-Myers Squibb, 5 Research Parkway, Wallingford, CT 06492 (USA)*

[++] *Current address: Shakti BioResearch, 1 Bradley Road, Suite 401, Woodbridge, CT 06525 (USA)*

[+++] *Currently at various functions within Bayer HealthCare Pharmaceuticals, Global Drug Discovery*

Supporting information for this article is available on the WWW under http://dx.doi.org/10.1002/cmdc.201300357.

  

ed with a plasmid containing four times the hypoxia response element of the VEGF promoter in front of a luciferase reporter gene construct. Cultivation of the cells under hypoxic conditions (1% $O_2$ for 16 h) led to hypoxia/HIF-induced expression of luciferase, which was suppressed by the test compounds to varying extents. Compound **1** (Figure 1) was found as the representative example of a confirmed hit cluster of 1*H*-pyrazole-3-carboxamides. It inhibits the luciferase signal with an $IC_{50}$ value of 190 nM.

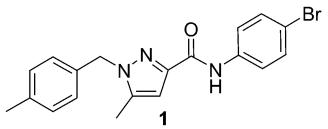


**1**

HIF–Luc $IC_{50}$: 190 ± 80 nM

**Figure 1.** Representative example from the screening hit cluster "1*H*-pyrazole-3-carboxamides". HIF–Luc $IC_{50}$: inhibitory potency in a cell-based reporter assay; see text and Experimental Section for explanations.

**Table 2.** Regiochemistry at the anilinic phenyl ring and its effect on HIF–Luc potency.

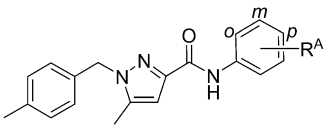


| Compd | $R^A$ | Regioisomer | $IC_{50}$ [nM][a] |
|---|---|---|---|
| **4** | –$OCF_3$ | *para* | 25 |
| **12** | –$OCF_3$ | *meta* | 5000 |
| **13** | –$OCF_3$ | *ortho* | >10000 |
| **14** | –*i*Pr | *para* | 39 |
| **15** | –*i*Pr | *meta* | 8100 |
| **16** | –*i*Pr | *ortho* | >10000 |
| **17** | –F | *para* | 150 |
| **18** | –F | *meta* | 890 |
| **19** | –F | *ortho* | 7200 |
| **20** | –Cl | *para* | 240 |
| **21** | –Cl | *meta* | 3200 |
| **22** | –Cl | *ortho* | 10000 |

[a] See footnotes in Table 1 for details.

Optimization of the screening hit started with variations of the *para* substituents of the anilinic and the benzylic phenyl rings, $R^A$ and $R^B$, both with respect to their chemical nature and their regiochemistry. The results for some of the $R^A$ analogues that we prepared are summarized in Tables 1 and 2; results for some of the $R^B$ analogues can be found in Table 3. A significant gain in potency was observed when the bromine was replaced by N-bound piperidine (compound **2**, 3.7 nM, Table 1). Other substituents led to more potent compounds as well. In general, it seems that bulky and/or lipophilic substituents $R^A$ increase potency, whereas more polar groups or less bulky substituents have the opposite effect (Table 1). There is a strong preference of $R^A$ for the *para* position, as is evident from the examples listed in Table 2.

The number of substituents $R^B$ investigated at the benzylic phenyl ring was smaller, and less SAR information was obtained. Apparently, there is only a weak preference for the *para* position over both *meta* and *ortho* (Table 3). We invested less effort into the optimization of $R^B$ at that stage, as we became aware of the hydrolytic instability of some of the 1*H*-pyrazole-3-carboxamides; we therefore redirected our attention from optimizing $R^B$ to addressing the stability issue. Cleavage of the amide bond was observed in vitro in rat plasma, which translated into above liver blood flow clearance in vivo (HTS hit **1**, Figure 2). We were able to replace the amide bond with an oxadiazole ring, which not only resolved the clearance problem, but also improved potency (compound **30**, Figure 2). Therefore, we abandoned the initial HTS structure class and turned our attention to further optimizing the new class of 5-(1*H*-pyrazol-3-yl)-1,2,4-oxadiazoles.

In the new series, the strong preference of the substituent $R^A$ (now attached to the oxadiazole-bound phenyl ring) for the *para* position was confirmed (Table 4), as was the weak prefer-

**Table 1.** Effect of the *para* substituent $R^A$ of the anilinic phenyl ring on HIF–Luc potency; representative examples out of 98 analogues in total.

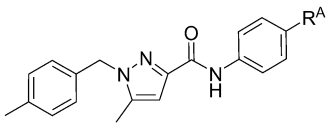


| Compd | $R^A$ | $IC_{50}$ [nM][a] | Compd | $R^A$ | $IC_{50}$ [nM][a] |
|---|---|---|---|---|---|
| **2** |  | 3.7 | **7** |  | 50 |
| **3** | –*t*Bu | 15 | **8** | –(CO)$NMe_2$ | 170 |
| **4** | –$OCF_3$ | 25 | **9** | –OMe | 220 |
| **5** | –*c*Hex | 36 | **10** | –$SO_2$Me | 330 |
| **6** | –$SF_5$ | 42 | **11** | –H | 460 |

[a] $IC_{50}$: inhibitory potency in the cell-based HIF–Luc reporter assay. The relative error of the $IC_{50}$ values is in the range of ±40%. See main text and Experimental Section for further explanations.

**Table 3.** Effect of the substituent $R^B$ of the benzylic phenyl ring on HIF–Luc potency.

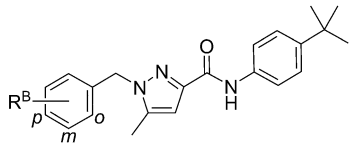


| Compd | $R^A$ | Regioisomer | $IC_{50}$ [nM][a] |
|---|---|---|---|
| **23** | MeO– | *para* | 11 |
| **24** | MeO– | *meta* | 29 |
| **3** | Me– | *para* | 15 |
| **25** | Me– | *ortho* | 14 |
| **26** | Cl– | *para* | 31 |
| **27** | H– | *para* | 37 |
| **28** | F– | *para* | 56 |
| **29** | *i*Pr– | *para* | 170 |

[a] See footnotes in Table 1 for details.

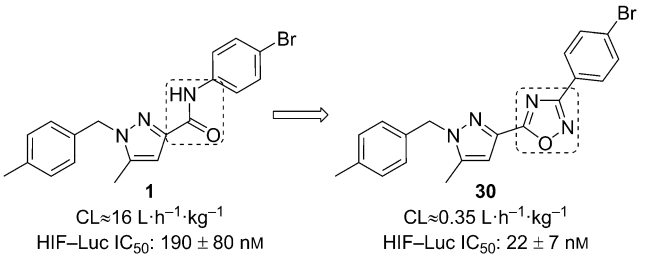


**Figure 2.** Strong decrease of in vivo clearance by replacement of the central amide bond with an oxadiazole ring in the screening hit **1**. CL: plasma clearance in mice after i.v. administration of 1 mg kg$^{-1}$ test compound.

**Table 4.** Regiochemistry at the oxadiazole-bound phenyl ring and its effect on HIF–Luc potency.

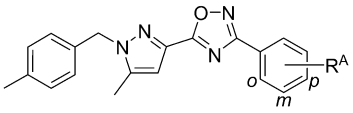


| Compd | $R^A$ | Regioisomer | $IC_{50}$ [nM][a] |
|---|---|---|---|
| **31** | $-CF_3$ | *para* | 40 |
| **32** | $-CF_3$ | *meta* | >10000 |

[a] See footnotes in Table 1 for details.

ence of $R^B$ likewise for *para* (Table 5). We then synthesized a number of analogues with different substituents in either *para* position: approximately 220 $R^A$ analogues and roughly 70 $R^B$ analogues were prepared and tested for their HIF–Luc potency. The results for some illustrative examples (with a certain bias for the more potent compounds) are listed in Tables 6 and 7.

The previously made observation holds true that bulky and lipophilic groups $R^A$ improve potency, whereas compounds with smaller substituents or polar groups (such as alcohols, amides, and carbamates) are less potent. The highest increase in potency was achieved with the 2,2,2-trifluoro-1,1-dimethylethyl derivative **36** (3 nM, first entry in Table 6) which was introduced as a potentially metabolically stable version of a *tert*-butyl group. At the benzylic phenyl ring, some polar substituents $R^B$ are well tolerated, whereas bulkiness seems not to be

**Table 5.** Regiochemistry at the benzylic phenyl ring and its effect on HIF–Luc potency in the oxadiazole series.

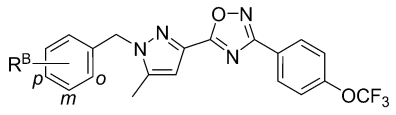


| Compd | $R^B$ | Regioisomer | $IC_{50}$ [nM][a] |
|---|---|---|---|
| ***33*** | **Me–** | ***para*** | **19±7** |
| **34** | Me– | *meta* | 100 |
| **35** | Me– | *ortho* | 500 |

[a] See footnotes in Table 1 for details.

**Table 6.** Effect of the substituent $R^A$ of the oxadiazole-bound phenyl ring on HIF–Luc potency; representative examples out of 220 analogues in total.

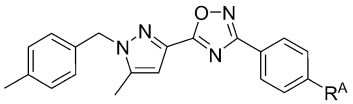


| Compd | $R^A$ | $IC_{50}$ [nM][a] | Compd | $R^A$ | $IC_{50}$ [nM][a] |
|---|---|---|---|---|---|
| **36** |  | 3 | **44** |  | 30 |
| **37** |  | 4 | **45** |  | 30 |
| **38** |  | 8 | **46** |  | 40 |
| **39** |  | 10 | **47** |  | 40 |
| **40** |  | 10 | **48** |  | 50 |
| **41** |  | 20 | **49** |  | 60 |
| **42** |  | 20 | **50** |  | 200 |
| **43** |  | 20 | **51** |  | 500 |

[a] See footnotes in Table 1 for details.

preferred. The methylamino derivative **52** (2 nM, first entry in Table 7) is tenfold more potent than the corresponding methyl analogue **33** (19 nM, first entry in Table 5). The rather low potencies of some of the analogues with ionizable groups may be due to their low target affinities, or may also be explained by a diminished ability to cross cell membranes (or both).

The combination of the two most potent substituents $R^A$ and $R^B$, i.e., 2,2,2-trifluoro-1,1-dimethylethyl of compound **36** (Table 6) and methylamino of compound **52** (Table 7), gave compound **62**, which is the most potent compound of the entire series, with a HIF–Luc $IC_{50}$ value of 0.7 nM (Figure 3).

Nevertheless, it was compound **33** (Table 5) that caught our attention very early during the course of the lead optimization, and we decided to investigate this compound in some detail. The ability of compound **33** to suppress HIF target gene expression in vitro was demonstrated by using human lung adenocarcinoma cell line A549, cultured under hypoxic conditions (1% $O_2$ for 16 h). In line with the $IC_{50}$ values on the reporter gene signal observed in the HCT-116 HIF–Luc screening cell line, compound **33** was also able to suppress hypoxia-induced gene expression in the non-transfected lung carcinoma cell line A549 at concentrations above 10 nM. Figure 4 displays the concentration-dependent decrease in mRNA levels of the HIF target genes CA-IX, EGLN-3, and VEGF, as quantified by RT-PCR. There is no effect of compound **33** on the expression level of the non-HIF target gene EGLN-2 (Figure 4). Additional gene expression data are available in the Supporting Information, as are western blots that show decreased HIF-1α and HIF-2α pro-

**Table 7.** Effect of the substituent $R^B$ of the benzylic phenyl ring on HIF–Luc potency; representative examples out of 70 analogues in total.

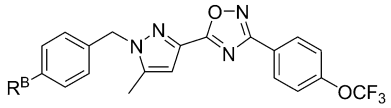

| Compd | $R^B$ | $IC_{50}$ [nM][a] | Compd | $R^B$ | $IC_{50}$ [nM][a] |
|---|---|---|---|---|---|
| **52** |  | 2 | **57** | 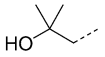 | 40 |
| **53** | 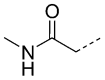 | 5 | **58** |  | 100 |
| **54** |  | 10 | **59** | 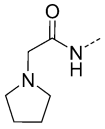 | 500 |
| **55** | 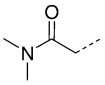 | 15 | **60** |  | 2000 |
| **56** |  | 40 | **61** | 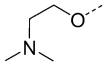 | 4000 |

[a] See footnotes in Table 1 for details.

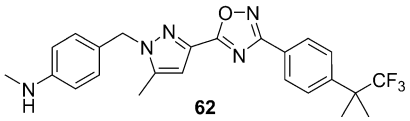

**62**
HIF–Luc $IC_{50}$: 0.7 ± 0.3 nM

**Figure 3.** The most potent compound of the lead series was derived from the initial screening hit **1** (Figure 1) by substitution of the amide bond for an oxadiazole ring, the introduction of a methylamino group in place of a methyl, and the introduction of a 2,2,2-trifluoro-1,1-dimethylethyl group replacing a bromine.

tein concentrations in the presence of compound **33**. A more detailed description of the pharmacology of compound **33** will be the subject of a separate communication.

Key pharmacokinetic properties of compound **33** are summarized in Table 8. After intravenous administration to rats, compound **33** displays low clearance and a very high volume of distribution, resulting in a long half-life of 30 h. When applied orally, the absolute bioavailability amounts to a favorable 74% and the half-life is, again, close to 30 h.

In conclusion, we have presented the discovery of compound **33** (HIF–Luc $IC_{50}$ = 19 nM) as a novel lead structure in the field of HIF pathway inhibitors. It was developed from the initial screening hit **1** (HIF–Luc $IC_{50}$ = 190 nM) by substitution of an amide bond for an oxadiazole ring and replacement of a bromine by a trifluoromethoxy group which improved the enzymatic hydrolytic stability significantly and increased potency.

Compound **33** suppresses hypoxia-induced expression of HIF target genes in vitro, whereas it does not have an effect on the expression levels of non-HIF target genes. The molecular target and thus the exact mode of action of compound **33** (and the entire pyrazolyl oxadiazole class) is currently under investigation. Compound **33** has a favorable pharmacokinetic profile in rat after intravenous and oral dosing. The structure–activity relationships reported herein show that further optimization of the lead is possible and likely promising, with compound **62** (HIF–Luc $IC_{50}$ = 0.7 nM) being the most potent member of the series to date.

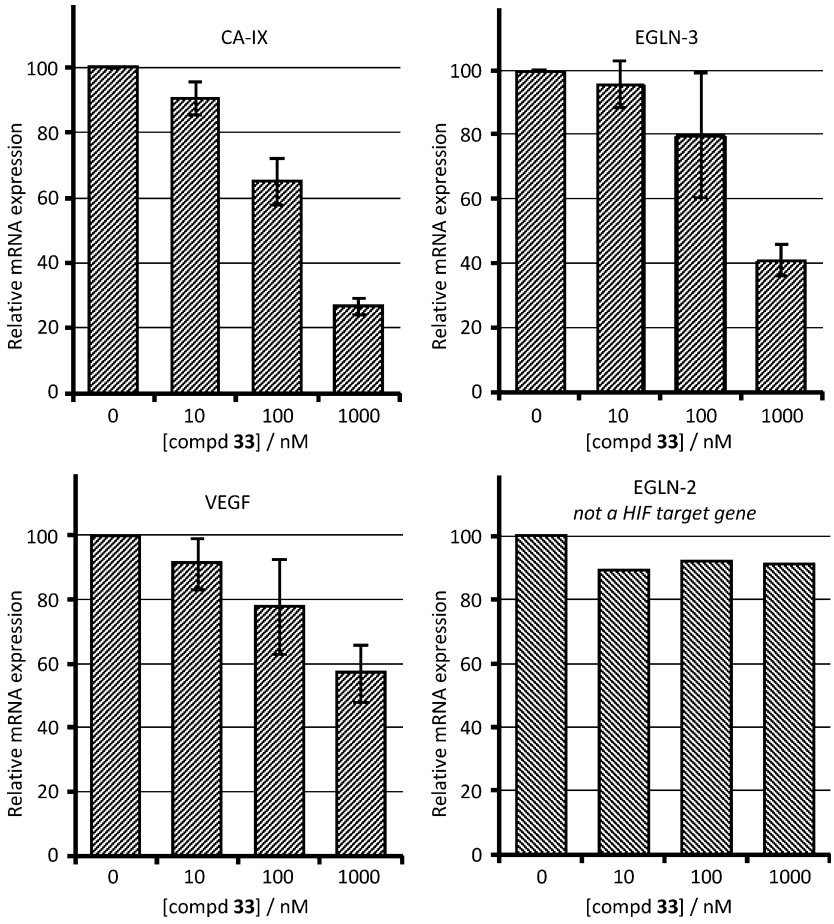


**Figure 4.** Effect of HIF pathway inhibitor **33** on the expression levels of HIF target genes (CA-IX, EGLN-3, and VEGF) and a non-HIF target gene (EGLN-2) in hypoxic A549 human lung adenocarcinoma cells. The cells were incubated for 16 h under hypoxic conditions (1% $pO_2$) with various concentrations of **33**. Gene expression was quantified by RT-PCR.

**Table 8.** Pharmacokinetic parameters of compound **33** after intravenous (i.v.) and oral (p.o.) application of solutions to rats.[a]

| Intravenous[b] [dose=0.36 mg kg$^{-1}$] | | Oral[b] [dose=3 mg kg$^{-1}$] | |
|---|---|---|---|
| $CL_{blood}$ [L h$^{-1}$·kg$^{-1}$] | 0.58 | $AUC_{norm}$ [kg h L$^{-1}$] | 1.92 |
| $V_{SS}$ [L kg$^{-1}$] | 6.9 | $C_{max,norm}$ [kg L$^{-1}$] | 0.16 |
| $t_{1/2}$ [h] | 30 | $t_{1/2}$ [h] | 29 |
| | | $F$ [%] | 74 |

[a] CL: clearance; $V_{SS}$: volume of distribution; $t_{1/2}$: half-life; $AUC_{norm}$: dose-normalized exposure (area under the curve); $C_{max,norm}$: dose-normalized maximum plasma concentration; $F$: absolute oral bioavailability. [b] 5 mL kg$^{-1}$ vehicle: plasma/DMSO = 98:2 (i.v.) or solutol/ethanol/water = 40:10:50 (p.o.).

## Experimental Section

*Chemistry*: Compound **33** was prepared in three steps from commercially available starting materials according to Scheme 1. Experimental details and analytical data are given in the Supporting Information, where the syntheses and analytical data of compounds **1**, **30**, and **62** can also be found.

*HIF–Luciferase assay*: Human colorectal carcinoma cells (HCT-116 cell line) were stably transfected with a plasmid containing a luciferase reporter under the control of an HIF-responsive sequence consisting of a fourfold repeat of the hypoxia-responsive element of the human VEGF promoter. These cells were sown in microtiter plates: 20000 cells per well in RPMI 1640 medium with 10% fetal calf serum (FCS) and 100 μg mL$^{-1}$ hygromycin. Incubation was carried out overnight under standard conditions: 21% $O_2$, 5% $CO_2$, 37 °C, humidified. The following morning, the cells were incubated with various concentrations of test substances (0–10 μM) in a hypoxia chamber with 1% $O_2$. After 24 h, Bright-Glo™ reagent (Promega, Wisconsin, USA) was added in accordance with the manufacturer's instructions, and after five minutes the luminescence was measured. Cells that were incubated under normoxic conditions served as background controls. Most $IC_{50}$ values given in this report are the average of two to four independent measurements and were rounded to two significant figures. The relative error of the $IC_{50}$ values is in the range of ±40% on average.

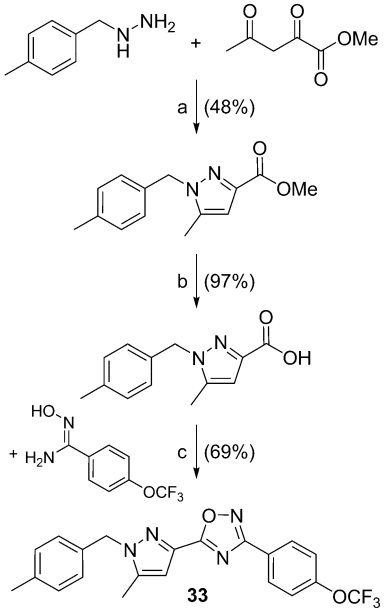


**Scheme 1.** Synthesis of compound **33**. *Reagents and conditions*: a) AcOH, 90 °C, 4 h, chromatographic separation of regioisomers (48% yield); b) NaOH (1 M in $H_2O$), EtOH, 70 °C, 15 h, acidification with $HCl_{(aq)}$ (97%); c) EDCI/HOBT, DMF, RT, 1 h, then 140 °C, 2 h (69%).

*Suppression of HIF target genes in vitro*: Human bronchial carcinoma cells (A549 cell line) were incubated for 16 h with variable concentrations of the test substances (0.001–10 μM) under either normoxic conditions or under 1% $O_2$ (see *HIF–Luciferase assay* above). The total RNA was isolated from the cells and transcribed into cDNA, and the mRNA expression of HIF target genes (and non-HIF target genes as controls) was analyzed by real-time PCR. mRNA expression levels of the HIF target genes are stronger under hypoxic conditions. Active test substances suppress the low constitutive mRNA expression levels of HIF target genes under normoxic conditions, but display a much stronger effect under hypoxic conditions. Expression levels of non-HIF target genes are unaffected by hypoxia and the presence of test compounds. Data are displayed as relative mRNA expression, for which the expression under hypoxic conditions and in the absence of test compound is set at 100%. Numbers of independent measurements: CA-IX (7), EGLN-3 (2), VEGF (2), EGLN-2 (1).

*Animal experiments*: All animal experiments were performed in accordance with German law on animal protection as revised in its current version. Permission is granted to Nonclinical Research Pharmacokinetics of Bayer Pharma AG by the animal protection agency of the state of North Rhine-Westphalia (Landesamt für Natur, Umwelt und Verbraucherschutz Nordrhein-Westfalen) to which the experiments had been notified.

## *Acknowledgements*

*The authors thank their co-workers for their dedicated and skillful work. Especially Karin Smyk, Peter Voits, Kirstin Seifert, Jana Wätzold, Sandra Zickelbein, Uwe Appel, Claus Jorzik, Philip Wickens, and Wenlang Fu, who conducted the chemical syntheses and carried out the HIF–Luc in vitro screen. The authors also thank Donald Bierer for the preparation of some parallel synthesis libraries, which helped to establish the early structure–activity relationships. The support by management functions (especially by Dieter Zopf, Michael Brands, Stefan Jaroch, Klaus Bosslet, Helmut Haning, and Karl Ziegelbauer) and the contributions by service functions of the various institutes are also gratefully acknowledged.*

**Keywords:** cancer · hit optimization · hypoxia-inducible factor (HIF) · inhibitors · transcription factors

[1] a) P. Vaupel, A. Mayer, *Cancer Metastasis Rev.* **2007**, *26*, 225–239; b) G. L. Semenza, *Oncogene* **2010**, *29*, 625–634.
[2] a) G. L. Semenza, G. L. Wang, *Mol. Cell. Biol.* **1992**, *12*, 5447–5454; b) G. L. Wang, G. L. Semenza, *J. Biol. Chem.* **1995**, *270*, 1230–1237.
[3] a) C. J. Schofield, P. J. Ratcliffe, *Nat. Rev. Mol. Cell Biol.* **2004**, *5*, 343–354; b) M. Ivan, K. Kondo, H. Yang, W. Kim, J. Valiando, M. Ohh, A. Salic, J. M. Asara, W. S. Lane, W. G. Kaelin, Jr., *Science* **2001**, *292*, 464–468; c) G. L. Semenza, *Physiology* **2009**, *24*, 97–106; d) Y. V. Liu, G. L. Semenza, *Cell Cycle* **2007**, *6*, 656–659; e) M. Y. Koh, T. R. Spivak-Kroizman, G. Powis, *Trends Biochem. Sci.* **2008**, *33*, 526–534; f) I. K. Nordgren, A. Tavassoli, *Chem. Soc. Rev.* **2011**, *40*, 4307–4317.

[4] a) A. Loboda, A. Jozkowicz, J. Dulak, *Mol. Cells* **2010**, *29*, 435 – 442; b) B. Keith, R. S. Johnson, M. C. Simon, *Nat. Rev. Cancer* **2012**, *12*, 9 – 22; c) S. M. Choi, H. Oh, H. Park, *FEBS J.* **2008**, *275*, 5618 – 5634; d) A. Ortiz-Barahona, D. Villar, N. Pescador, J. Amigo, L. del Peso, *Nucleic Acids Res.* **2010**, *38*, 2332 – 2345.

[5] a) K. Hirota, G. L. Semenza, *Crit. Rev. Oncol. Hematol.* **2006**, *59*, 15 – 26; b) M. J. Calzada, L. del Peso, *Clin. Transl. Oncol.* **2007**, *9*, 278 – 289; c) G. L. Semenza, *Semin. Cancer Biol.* **2009**, *19*, 12 – 16; d) H. Harada, M. Hiraoka, *Curr. Signal Transduction Ther.* **2010**, *5*, 188 – 196; e) N. M. Mazure, M. C. Brahimi-Horn, J. Pouysségur, *Bull. Cancer* **2011**, *98*, 40 – 46; f) N. Rohwer, T. Cramer, *Drug Resist. Updates* **2011**, *14*, 191 – 201.

[6] a) H. S. Ban, Y. Uto, H. Nakamura, *Expert Opin. Ther. Pat.* **2011**, *21*, 131 – 146; b) Y. Xia, H.-K. Choi, K. Lee, *Eur. J. Med. Chem.* **2012**, *49*, 24 – 40; c) D. T. Jones, A. L. Harris, *Expert Opin. Ther. Targets* **2012**, *16*, 463 – 480; d) R. Wang, S. Zhou, S. Li, *Curr. Med. Chem.* **2011**, *18*, 3168 – 3189; e) Y. Hu, J. Liu, H. Huang, *J. Cell. Biochem.* **2013**, *114*, 498 – 509; f) H. Minegishi, T. Matsukawa, H. Nakamura, *ChemMedChem* **2013**, *8*, 265 – 271.

[7] R. B. Cohen, A. Olszanski, J. Figueroa, H. Hurwitz, F. M. Lokiec, K. Rezai, N. B. Berkowitz, A. Buchbinder, *American Association for Cancer Research (AACR) 102nd Annual Meeting*, April 2 – 6, **2011**, (Orlando, FL, USA), Abstract LB-407.

Received: September 6, 2013
Revised: November 8, 2013
Published online on November 27, 2013